Available online at www.sciencedirect.com

ScienceDirect

Journal of Nuclear Materials 359 (2006) 114–121

journal of nuclear materials

www.elsevier.com/locate/jnucmat

Influence of hydrogen on the toughness of irradiated reactor pressure vessel steels

G. Müller [a,*], M. Uhlemann [b], A. Ulbricht [a], J. Böhmert [a]

[a] *Forschungszentrum Rossendorf e.V., Institut für Sicherheitsforschung, P.O. Box 510119, 01314 Dresden, Germany*
[b] *Institut für Festkörper- und Werkstoffforschung Dresden, P.O. Box 270016, 01171 Dresden, Germany*

Received 1 February 2006; accepted 14 August 2006

Abstract

The influence of hydrogen on the mechanical behaviour of different reactor pressure vessel (RPV) steels was investigated by tensile tests in correlation to the chemical composition, the neutron fluence, the hydrogen charging condition, the strain rate, and the temperature. Small-angle neutron scattering (SANS) experiments, hydrogen analyses and thermal desorption investigations were performed to prove the evidence of hydrogen trapping at irradiation defects. An increasing susceptibility to hydrogen embrittlement indicated by reduction of area was observed at room temperature with in situ hydrogen-charged specimens when loaded by low strain rates or with specimens which had been irradiated at low temperature. Generally, the susceptibility increases with increasing strength of the steels. At 250 °C hydrogen embrittlement was not evident. The results do neither prove that irradiation defects are favoured traps for hydrogen nor give evidence that hydrogen affects the RPV integrity under normal operating conditions.

1. Introduction

The embrittlement of RPV steels is caused by nanodispersed structural defects formed during the operation of a nuclear pressure vessel by neutron irradiation. It depends on the operational conditions as well as the type and the chemical composition of the RPV steel. On the other hand, hydrogen also influences the deformation behaviour of steel and it is not excluded that synergistic effects between neutron and hydrogen embrittlement are effective [1–3]. For example, the uptake of hydrogen and an enhanced susceptibility for embrittlement were proved for irradiated steels with austenitic claddings under RPV conditions [4]. Splichal et al. [4,5], Brinkman and Beston [6] and Takaku et al. [7,8] specified critical hydrogen concentrations of $\geqslant$2.5–4 wt ppm for degradation of the mechanical properties both in the unirradiated and the irradiated condition. Kimura et al. [9] proved that the critical hydrogen charging current density of neutron-irradiated martensitic steel was smaller than that of unirradiated one. From increased crack growth rates measured under service conditions after hydrogen pre-charging of unirradiated RPV steel, Lee et al. [10] showed that hydrogen is also

* Corresponding author. Tel.: +49 351 260 2149; fax: +49 351 260 2205.
E-mail address: g.mueller@fz-rossendorf.de (G. Müller).

0022-3115/$ - see front matter © 2006 Elsevier B.V. All rights reserved.
doi:10.1016/j.jnucmat.2006.08.004

trapped at structural defects at operating temperatures. These defects can act as internal hydrogen sources and thus, cause increased embrittlement. Wu and Katada [11–13] investigated the low-cycle fatigue behaviour, fatigue crack initiation and growth behaviour of unirradiated low-alloy pressure vessel steel A533B in a simulated BWR (boiling water reactor) environment. They could prove a close strain rate dependence of the cyclic cracking morphologies in high-temperature water, due to a change in the dominant environmentally assisted cracking. Investigations of Krasikov and Amajev [14] on irradiated steels after alternating hydrogen charging and annealing led to an evident degradation of the plasticity of the material. However, crack growth investigations performed in the nuclear research centre of Rež [15] under the simultaneous influence of simulated BWR coolant and irradiation did not show an increased environmentally assisted crack growth compared to unirradiated specimens. Seifert et al. [16] assumed that a hydrogen-induced damage mechanism at LWR operation temperature hardly exists because of the high diffusion rate of hydrogen and the small trap efficiency.

Small-angle neutron scattering (SANS) has proved to be an effective method to investigate microstructural defects induced by neutron irradiation [17–20]. The enrichment of hydrogen within the nuclear structural defects can be indicated by SANS because hydrogen increases the nuclear scattering contrast whereas the magnetic component remains unaffected [21]. SANS measurements on irradiated RPV steels with subsequent hydrogen charging were already published in [22].

The paper reports about investigations of the influence of hydrogen on the mechanical behaviour of irradiated RPV steels by tensile tests in correlation to the chemical composition, the neutron fluence, the hydrogen charging condition, the strain rate, and the temperature. SANS experiments, hydrogen analyses and thermal desorption investigations were performed to prove the evidence of hydrogen trapping at irradiation defects [23,24].

2. Experimental methods

2.1. Material and irradiation conditions

The materials and irradiation conditions are given in Tables 1 and 2. The steels with the codes JPA and JRQ are materials from the IAEA-CRP programme, phase 3. They are nickel containing RPV steels according to ASTM standard. KAB is a nickel poor and vanadium alloyed Russian RPV steel that was used for the first VVER-440 generation. Skoda designated a VVER-440 RPV steel from Czech production. All materials are base metals. The irradiation experiments were executed in the VVER-2 prototype reactor in Rheinsberg (Germany). The operation temperature was 255 °C. Only the

Table 1
Chemical composition of materials (mass%, Fe balance)

Type	Code	C	Si	Mn	Cr	Ni	Mo	V	S	P	Cu
A533B Cl.1	JRQ	0.19	0.29	1.41	0.12	0.84	0.50	–	0.004	0.019	0.14
A508 Cl.3	JFL	0.17	0.25	1.44	0.20	0.75	0.51	0.004	0.002	0.004	0.01
15Kh2MFA	KAB	0.14	0.24	0.55	2.60	0.24	0.62	0.270	0.013	0.011	0.22
15Kh2MFA	Skoda	0.17	0.38	0.54	2.98	0.10	0.73	0.370	0.016	0.019	0.09

Table 2
Irradiation conditions of materials

Material code	Reactor	Temp. (°C)	Irradiation experiment	Fluence ($E > 0.5$ MeV) (10^{18} cm^{-2})	Δc^{a} (vol.%)
JRQ	VVER-2 Rheinsberg	255	RH-6	10.8	0.206
			RH-7	125	0.502
JFL	VVER-2 Rheinsberg	255	RH-6	9	0.003
			RH-7	81	0.020
			RH-7	139	0.086
KAB	VVER-2 Rheinsberg	255	RH-7	139	0.268
KAB-(8)	RFR Rossendorf	>60	RFR	20	0.07
Skoda	VVER-2 Rheinsberg	255	RH-8	4.6	–

[a] Volume fraction of radiation defects.

material KAB-(8) (layer 8 of the KAB material) was irradiated in the Rossendorf Research Reactor RFR at an operational temperature of about 60 °C. More details about materials, irradiation and microstructure are given in [25].

2.2. Test methods

The specimens were cathodically charged in simulated RPV water containing 0.1 M boric acid/0.01 M KOH with current densities of -5 mA/cm^2 up to saturation at room temperature (RT). The aim of the charging was not to achieve a very high hydrogen concentration but to realize conditions like in a pressure water reactor. Whereas one part of the specimens, unirradiated as well as irradiated, was only hydrogen pre-charged immediately before tensile testing, the other part was additionally charged in situ during the tensile tests.

The uniaxial tensile tests were performed in a hot cell with a servo-hydraulic test system MTS 810/50 kN at RT and 250 °C and at strain rates $d\varepsilon/dt = 10^{-4}\ s^{-1}$ and $d\varepsilon/dt = 10^{-6}\ s^{-1}$. Sub-size tensile specimens were used for the tests, depicted in Fig. 1. The hydrogen in situ charging was realized by a specially constructed device, which enabled simultaneous hydrogen charging and mechanical testing. The in situ tests were only performed at RT.

The fracture surfaces of the tensile specimens were investigated by SEM, DMS 962 Zeiss. For irradiated specimens a special replica technique was developed [26]. This technique does not conserve every small detail of the fracture surface but it permits to clearly distinguish the type of fracture.

The hydrogen content was immediately determined after hydrogen charging by hot-extraction with the hydrogen analyzer HORIBA EMGA 621B. Slices of 0.8 mm thickness and 8×4 mm size were used. The materials were tested in the unirradiated and in the irradiated condition and in the non-charged state as well as after hydrogen charging. The temperature dependent effusion behaviour was measured by thermal desorption, performed 24 h after hydrogen charging. At this time the diffusible hydrogen was effused from the material and only the trapped hydrogen could be detected. In ultra-high vacuum the specimens were heated at a heating rate of 14.7 K/min and the effused hydrogen was detected by mass spectrometry (Transpector/Leybold).

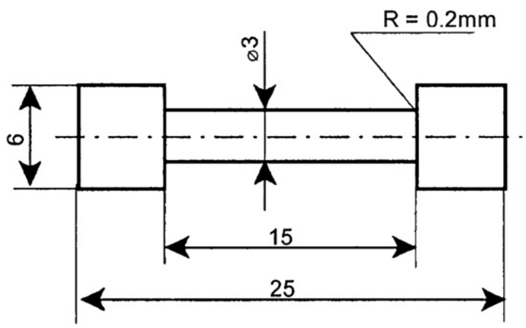

Fig. 1. Small tensile specimen.

The SANS experiments were executed with the spectrometer V4 of HMI Berlin [27]. The experimental details and results are published in [22].

3. Results and discussion

3.1. Tensile tests and fractography

Tensile strength R_m and yield strength $R_{p0,2}$ are not influenced by hydrogen pre-charging or in situ charging. However, significant differences are observed at the toughness parameters like elongation after fracture and in particular at the reduction of area for all steels in the unirradiated and irradiated conditions when the specimens are hydrogen-charged during the tensile tests. This is shown in Fig. 2 for the steels in the unirradiated condition. Whereas pre-charging hardly changes the reduction of area, the parameter is clearly reduced by in situ charging. This is especially evident for the lower strain rate of $10^{-6}\ s^{-1}$. Wu and Kim [28] obtained similar tensile test results at RT for unirradiated

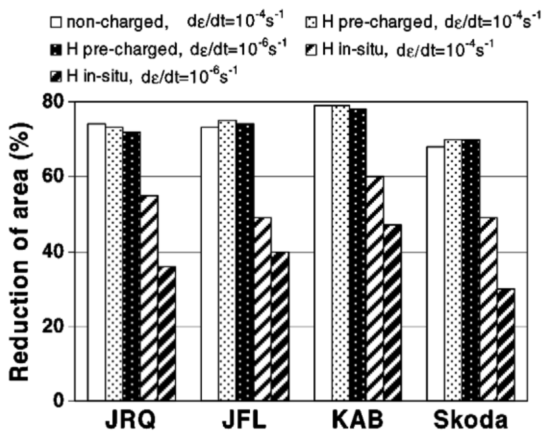

Fig. 2. Reduction of area of unirradiated specimens for different hydrogen charging and test conditions at RT.

SA508 Cl.3, but they observed the strong strain-rate dependence of ductility already after hydrogen pre-charging. It is assumed that electroplating with copper after cathodic hydrogen charging suppresses hydrogen desorption and so the hydrogen content during the tensile test may be comparable to that of our in situ charged specimens. In accordance with our results they observed only a small influence of hydrogen on the tensile strength but a decrease of ductility with the decrease in strain rate. The effect of irradiation and hydrogen charging is shown in Figs. 3 and 4. As known, irradiation decreases the reduction of area, but not dramatically. In connection with the in situ hydrogen charging the decrement is substantial and increases with increasing neutron fluence. In the case of the material JRQ a total embrittlement with a value of the reduction of area of only about 5% is reached after neutron exposition of 125×10^{18} cm^{-2}. For the other materials, the reduction of area remains at about 20% for similar neutron exposure. Note, the material JRQ is considered to be especially susceptible to neutron embrittlement.

The SEM micrographs support this result. Some examples are given in Figs. 5–7. Fig. 5 shows the fracture surface of an unirradiated tensile specimen, hydrogen pre-charged and tested at slow strain rate $d\varepsilon/dt = 10^{-6}$ s^{-1} and RT. The microstructure is characterized by a ductile dimple fracture. However, in the fracture surface of an irradiated pre-charged

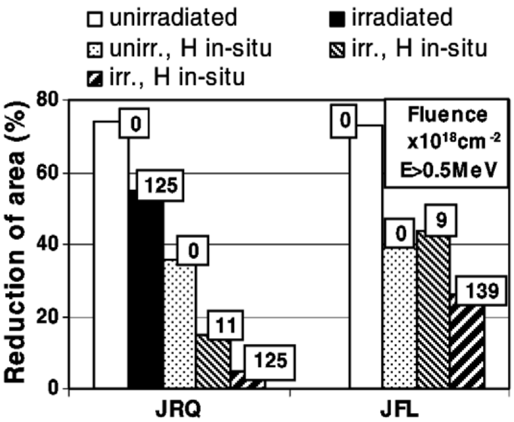

Fig. 3. Reduction of area of hydrogen in situ charged specimens (JRQ, JFL, $d\varepsilon/dt = 10^{-6}$ s^{-1}, RT) for different fluences (numbers in the boxes), compared to non-charged unirradiated and irradiated specimens.

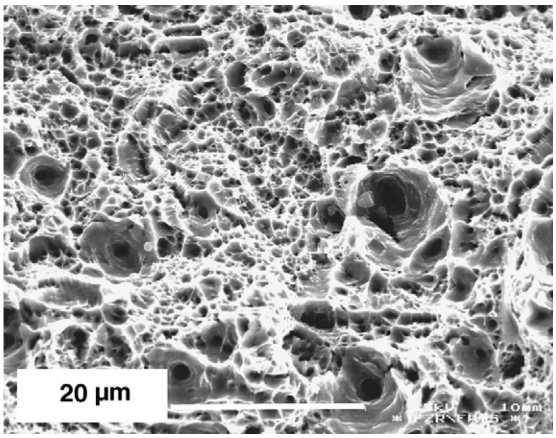

Fig. 5. SEM, fracture surface of an unirradiated JRQ tensile specimen, hydrogen-pre-charged, strain rate $d\varepsilon/dt = 10^{-6}$ s^{-1}.

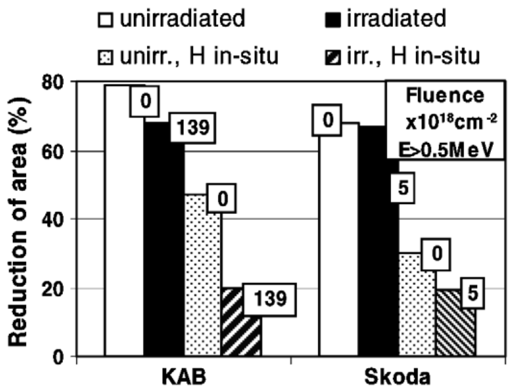

Fig. 4. Reduction of area of hydrogen in situ charged specimens (KAB, Skoda, $d\varepsilon/dt = 10^{-6}$ s^{-1}, RT) for different fluences (numbers in the boxes), compared to non-charged unirradiated and irradiated specimens.

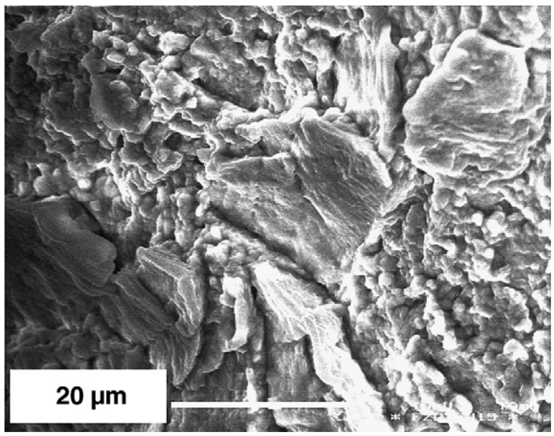

Fig. 6. SEM, fracture surface of an irradiated JRQ tensile specimen, hydrogen-pre-charged, strain rate $d\varepsilon/dt = 10^{-6}$ s^{-1}.

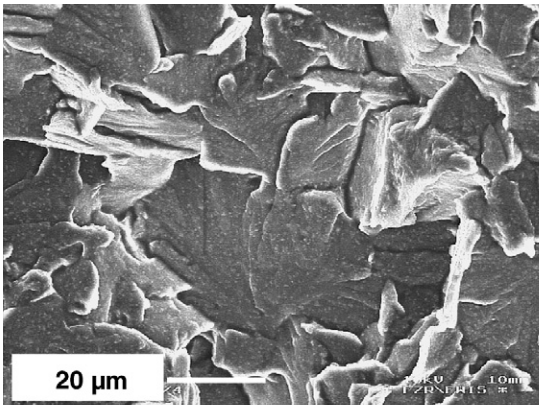

Fig. 7. SEM, fracture surface of an irradiated JRQ tensile specimen, hydrogen in situ charged, strain rate $d\varepsilon/dt = 10^{-6}\ s^{-1}$.

specimen, deformed at the same strain rate and temperature, a mixed fracture can be seen, consisting of dimple and cleavage fracture, see negative replica in Fig. 6. The fracture surface of an irradiated in situ charged specimen, negative replica in Fig. 7, is characterized by transcrystalline cleavage fracture with parts of intergranular brittle fracture. All fracture surfaces of the other materials show mixed fracture after hydrogen in situ charging.

The reduction of area versus the tensile strength is shown in Fig. 8 for all materials. One can see an approximately linear decrease of the reduction of area with increasing tensile strength independent of the type of material or the irradiation state. Strain rate had no effect on this relation in non-charged and pre-charged specimens, but in in situ charged specimens. The reason may be that hydrogen charged before testing is able to effuse from the steel at RT and so hydrogen is not effective during the tensile test. Thus, the deformation behaviour of pre-charged specimens does not reflect the real behaviour under the condition of spontaneous hydrogen supply like in situ charging. For in situ charging the slope of the line for the reduction of area versus tensile strength is similar for both tested strain rates, but the line of the lower strain rate is clearly shifted to lower values of the area reduction. The strong decrease of toughness, especially at the low strain rate, is observed both for unirradiated and irradiated specimens with in situ hydrogen charging. This result suggests that the enhanced area reduction of irradiated steels, i.e., the higher susceptibility against hydrogen embrittlement is only caused by hardening due to radiation defects. There are no hints that irradiation-induced defects are favoured traps for hydrogen.

It has to be pointed out, that the results of the material KAB-(8) are not included in Fig. 8. This test series is different to all the others because of the different irradiation temperature of about 60 °C. The tensile strength and the yield stress are approximately equal after irradiation. In contrast to the mentioned results, the toughness decreases already after hydrogen pre-charging as seen in Fig. 9. Obviously, there are hydrogen traps of higher efficiency, which fix the hydrogen atoms at RT. According to references [25,29] the microstructural defects after low temperature irradiation consist of very small vacancy clusters. A strong interaction between hydrogen and such vacancy clusters can be assumed and was proved by Lee et al. for micro-voids [30].

The tensile tests in irradiated steels at 250 °C were exclusively performed after hydrogen pre-

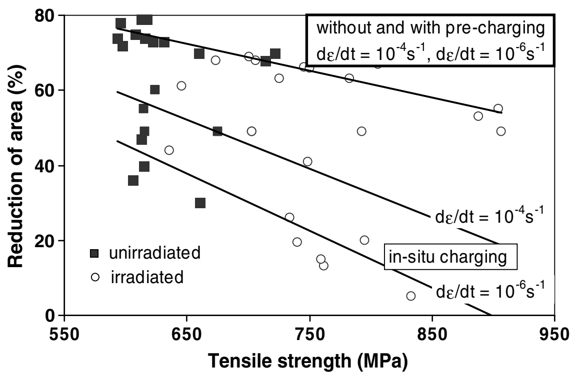

Fig. 8. Reduction of area in correlation to the tensile strength of unirradiated, irradiated, non-charged, hydrogen-pre-charged and in situ charged specimens for different strain rates and at RT.

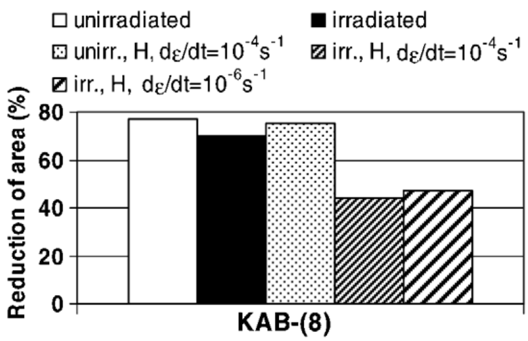

Fig. 9. Reduction of area of unirradiated, irradiated, non-charged and hydrogen-pre-charged specimens (KAB-(8)) for different strain rates and at RT.

charging. Strength and toughness parameters of unirradiated and irradiated steels decrease at 250 °C in comparison to RT, with no apparent effect of hydrogen pre-charging. All fracture surfaces are characterized by dimple fracture [24]. Unirradiated steels were also tested at 250 °C under in situ charging conditions. The results do not show changes of strength or toughness properties in comparison to the tests in the non-charged or hydrogen pre-charged conditions [23]. Lee and Kim [31] also showed only a small effect of hydrogen on ultimate tensile strength and ductility loss for unirradiated, hydrogen pre-charged SA508 Cl.3 at a comparable strain rate at 250 °C, but in contrast to Lee and Kim, we observed the effect of dynamic strain aging already at 250 °C and at lower strain rates. Lee and Kim [31] as well as Wu and Kim [28] proved that observable hydrogen effects appeared at higher strain rates ($d\varepsilon/dt = 10^{-3}\ s^{-1}$) at higher temperatures (288 °C).

In the case of the material KAB-(8), irradiated at low temperature, the strength parameters also decrease at 250 °C in comparison to RT, but the toughness parameters of irradiated, pre-charged steels increase at 250 °C [24]. This could be the result of an annealing effect already at low temperatures on the vacancy-rich defects.

3.2. Hydrogen analysis and thermal desorption investigations

The results of the hydrogen content measurements of specimens in the as-received condition and after charging are shown in Table 3. Compared with unirradiated JRQ the hydrogen content after charging is by 1.7 wt ppm higher in the irradiated condition. There is no difference of hydrogen content between the unirradiated and irradiated condition for the material Skoda, the hydrogen content amounts to about 3 wt ppm. The determination of differently bonded hydrogen by means of thermal desorption measurements is shown in Figs. 10 and 11. Small amounts of hydrogen are strongly bonded

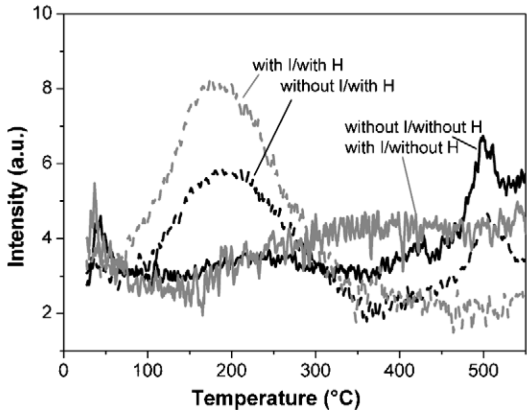

Fig. 10. Thermal desorption investigation of JRQ in the unirradiated and irradiated conditions, non-charged and hydrogen-pre-charged.

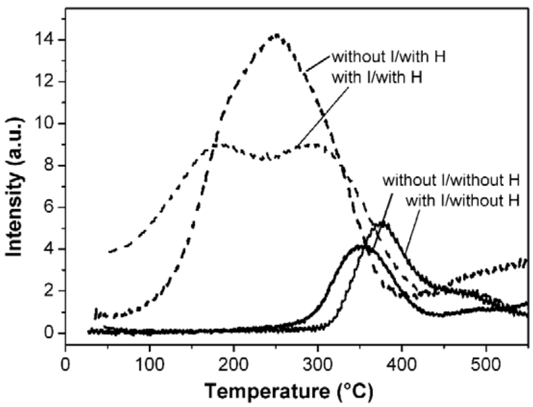

Fig. 11. Thermal desorption investigation of Skoda in the unirradiated and irradiated conditions, non-charged and hydrogen-pre-charged.

already in the non-charged steels (unirradiated and irradiated). Small effusion peaks are not observed until 300 °C. A second peak appears with a maximum at 200 °C after hydrogen charging, but the effusion starts always below 100 °C. This means that additional hydrogen is only weakly bonded at microstructural defects, which already exist in the

Table 3
Hydrogen content of the unirradited and irradiated materials JRQ and Skoda, charging conditions: $i = -5\ mA/cm^2$, RT

Mat. code (irradiation exp.)	Electrolyte	Unirradiated non-charged (wt ppm)	Unirradiated pre-charged (wt ppm)	Irradiated non-charged (wt ppm)	Irradiated pre-charged (wt ppm)
JRQ (RH-6)	Boric acid/KOH	0.39	2.02	–	3.72
Skoda (RH-8)	$NaOH+As_2O_3$	0.50... (2.0)	3.10	0.95	2.87

unirradiated steel. The slightly higher peak of the irradiated and charged JRQ steel correlates to the results of the hydrogen content measurements, given in Table 3. This result and the splitted effusion peak of the irradiated and charged Skoda material could be a hint, that hydrogen is bonded at different kinds of defects which could be formed during irradiation.

3.3. SANS investigations

The SANS measurements show that hydrogen trapping at small microstructural heterogeneities can even be identified if the bulk concentration of hydrogen is not higher than 1–2 wt ppm [22]. Hydrogen charging enhances the nuclear component of the small-angle scattering. The hydrogen trapping effect depends on the type of material. Preferential hydrogen traps are microstructural heterogeneities of sizes between 8 and 20 nm but also smaller ones. This result points to small carbides with coherent or semi-coherent interfaces [25,32]. However, the characteristic radiation defects in the size range of about 1 nm seem to be not effective as hydrogen traps [22]. The SANS results correspond to the results of the tensile tests.

4. Conclusion

Hydrogen uptake during simultaneous tensile loading results in a reduction of the toughness proved by reduction of the area to fracture of RPV steels whereas the strength parameters hardly changed. The toughness reduction is especially significant for low strain rates, e.g. $d\varepsilon/dt = 10^{-6}\ s^{-1}$. The effect is not critical for the steels in the unirradiated condition, at least as long as the hydrogen uptake is not higher than a few wt ppm. However, hydrogen induced embrittlement adds up to the neutron irradiation-induced reduction of the toughness (neutron embrittlement). In the case of high neutron fluence and material with high susceptibility to neutron embrittlement, a nearly total loss of toughness can occur. It is characterized by complete cleavage fracture and values of an area reduction of only few percents. The result is not a consequence of an interaction between irradiation-produced microstructural defects and the hydrogen atoms as proved by SANS. It is rather the consequence of the well-known fact that the susceptibility to hydrogen embrittlement increases with increasing strength of the steel.

Irradiation at lower temperatures can produce special types of microstructural defects like vacancy clusters that have a higher trend to bind hydrogen. In such cases a synergistic effect cannot be excluded.

Eventually, the experiments do not give an unambiguous prediction on the behaviour under operational conditions of a reactor. Tensile tests on irradiated specimens at temperatures comparable with reactor operation temperatures are only performed with hydrogen pre-charging. In this case, hydrogen is probably completely removed before testing.

Acknowledgements

The work was sponsored by the Bundesministerium für Wirtschaft und Arbeit under contract GRS 1501267. The authors are grateful for the sponsorship.

References

[1] J.P. Hirth, Metall. Trans. 11A (1989) 861.
[2] D. Pachur, in: Effects of radiation on materials: 18th International Symposium, Hyannis, MA, USA, June 22–25, 1996.
[3] H. Hänninen, in: 20th meeting of AMES Steering Committee, Paris, March 2000, unpublished.
[4] K. Splichal, M. Ruscak, M. Zdarek, J. Press. Vessel Piping 55 (1993) 3361.
[5] J. Koutsky, K. Splichal, Met. Mater. 23 (1985) 252.
[6] C.R. Brinkman, J.M. Beeston, in: Irradiation effects on structural alloys for nuclear reactor applications, ASTM STP 484 (1970) 42.
[7] H. Takaku, H. Kayano, J. Nucl. Mater. 110 (1982) 286.
[8] H. Takaku, H. Kayano, J. Nucl. Mater. 78 (1978) 299.
[9] A. Kimura, H. Kayano, M. Narui, J. Nucl. Mater. 179–181 (1991) 737.
[10] S.G. Lee, I.S. Kim, in: Proceedings of 11th International Conference on Environmental Degradation of Materials in Nuclear Systems, Stevenson, WA, August 10–14 (2003) 126.
[11] X. Wu, Y. Katada, J. Nucl. Mater. 328 (2004) 115.
[12] X. Wu, Y. Katada, Corros. Sci. 47 (2005) 1415.
[13] X. Wu, Y. Katada, Mater. Corros. 56 (2005) 305.
[14] E.A. Krasikov, A.D. Amajev, J. Nucl. Mater. 283–287 (2000) 846.
[15] G. Brümmer, H. Hoffmann, F. Hütten, U. Ilg, O. Wachter, M. Widera, A. Brozova, J. Burda, O. Erben, M. Ernestova, J. Kysela, M. Postler, R. Vsolak, in: Proceedings of the 11th International Conference on Environmental Degradation of Materials in Nuclear Systems, Stevenson, WA, August 10–14 (2003) 116.
[16] H.P. Seifert, S. Ritter, J. Hickling, in: Proceedings of the 11th International Conference on Environmental Degradation of Materials in Nuclear Systems, Stevenson, WA, August 10–14 (2003) 73.

[17] G. Solt, F. Frisius, W.B. Weaber, P. Tipping, in: Effects of Radiation on Materials, ASTM STP 1175 (1993) 444.
[18] W.J. Phytian, C.A. English, J. Nucl. Mater. 205 (1993) 162.
[19] B.D. Wirth, G.R. Odette, P.A. Pavinich, G.E. Lucas, S.E. Spooner, in: Effects of Radiation on Materials, ASTM STP 1325 (1999) 102.
[20] A. Ulbricht, J. Böhmert, H.-W. Viehrig, P. Strunz, C. Dewhurst, M. Mathon, Appl. Phys. A 74 (2002) S1128.
[21] L. Koester, H. Rauch, E. Seymann, Atom. Data Nucl. Data Tables. 49 (1991) 65.
[22] A. Ulbricht, J. Böhmert, M. Uhlemann, G. Müller, J. Nucl. Mater. 336 (2005) 90.
[23] M. Uhlemann, J. Böhmert, G. Müller, Einfluss von Wasserstoff auf die Zähigkeitsabnahme von RDB-Stählen, BMWA-Abschlussbericht IFW Dresden, 2001.
[24] M. Uhlemann, G. Müller, A. Ulbricht, J. Böhmert, Einfluss von Wasserstoff auf die Zähigkeitsabnahme von bestrahlten RDB-Stählen, BMWA-Abschlussbericht IFW Dresden, 2004.
[25] J. Böhmert, A. Gokhman, M. Große, A. Ulbricht, Nachweis, Interpretation und Bewertung bestrahlungsbedingter Gefügeänderungen in WWER-Reaktordruckbehälterstählen, Forschungszentrum Rossendorf, Wiss.-techn. Bericht FZR-381, 2003.
[26] G. Müller, Praktische Metallographie 35 (2004) 371.
[27] U. Kleiderling, A. Wiedemann, Physica B 213&214 (1995) 835.
[28] X.Q. Wu, I.S. Kim, Mat. Sci. Eng. A 348 (2003) 309.
[29] G. Brauer, L. Liszkay, B. Molnar, R. Krause, Nucl. Eng. Design 127 (1991) 47.
[30] J.Y. Lee, S.M. Lee, Surface Coating Technol. 28 (1986) 301.
[31] S.G. Lee, I.S. Kim, Mat. Sci. Eng. A 420 (2006) 279.
[32] N. Paroathavarthini, S. Saroja, R.K. Dayal, H.S. Khatak, J. Nucl. Mater. 288 (2001) 187.